2005-05-04

Overexpression of cytochrome P450 1A1 and its novel spliced variant in ovarian cancer cells: alternative subcellular enzyme compartmentation may contribute to carcinogenesis

Yuet-Kin Leung
University of Massachusetts Medical School

Et al.

Overexpression of *Cytochrome P450 1A1* and Its Novel Spliced Variant in Ovarian Cancer Cells: Alternative Subcellular Enzyme Compartmentation May Contribute to Carcinogenesis

Yuet-Kin Leung,[1] Kin-Mang Lau,[1] James Mobley,[1] Zhong Jiang,[2] and Shuk-Mei Ho[1,3,4]

Departments of [1]Surgery, [2]Pathology, [3]Cell Biology, and [4]Physiology, University of Massachusetts Medical School, Worcester, Massachusetts

Abstract

Epithelial ovarian cancer derived from the human ovarian surface epithelium (HOSE) is the leading cause of death from gynecologic malignancies among American women. Metabolic activation of endogenous and exogenous chemicals by cytochrome *P*450 (CYP) class I enzymes has been implicated in its etiology. In this study, we showed overexpression of *CYP1A1* mRNA, but not *CYP1B1* transcripts, in ovarian cancer cell lines when compared with primary cultures or immortalized HOSE cell lines. Importantly, we identified a novel, enzymatically active, spliced variant of *CYP1A1* (*CYP1A1v*) formed by excision of an 84-bp cryptic intron in exon 2. *CYP1A1v* is overexpressed in ovarian cancer cell lines and exhibits a unique subcellular distribution restricted to the nucleus and mitochondria, contrary to the endoplasmic reticulum localization of the wild-type enzyme. In concordance, total CYP1A1 activity, as measured by the ethoxyresorufin *O*-deethylase assay, was detected in mitochondrial, nuclear, and microsomal fractions of ovarian cancer cells but was notably absent in all subcellular fractions of HOSE cells. Immunocytochemistry studies in 30 clinical specimens revealed overexpression of CYP1A1 in various types of ovarian cancers compared with benign epithelia and frequent localization of the enzyme to cancer cell nuclei. Forced expression of *CYP1A1wt* or *CYP1A1v* in HOSE cells resulted in nuclear localization of the enzyme and acquisition of anchorage-independent growth, which was further exacerbated following exposure to benzo(*a*)pyrene or 17β-estradiol. Collectively, these data provided the first evidence that *CYP1A1* overexpression and alternative splicing could contribute to ovarian cancer initiation and progression. (Cancer Res 2005; 65(9): 3726-34)

Introduction

In the United States, ovarian cancer is the leading cause of death from gynecologic neoplasms (1). About 23,000 cases are diagnosed each year and 14,000 women die from the disease. The majority (≈90%) of ovarian cancers are epithelial cancers arising from the human ovarian surface epithelium (HOSE), which is a simple squamous-to-cuboidal mesothelium covering the ovary.

Epidemiologic studies suggest dietary/environmental factors, such as high levels of meat consumption (2), caffeine intake (3), and cigarette smoking (4), are risk factors for ovarian cancer. In these instances, cytochrome *P*450 (CYP) 1A1 may play a major role in the metabolic activation of procarcinogens to carcinogens. For example, it is known that polycyclic aromatic hydrocarbons (PAH), by-products of incomplete combustion and pyrolysis of fossil fuels and organic matters, such as tobacco leaf, are direct carcinogens of HOSE cells (5). Other environmental pollutants, such as the halogenated aryl hydrocarbon 2,3,7,8-tetrachlorodibenzo-*p*-dioxin (TCDD), a by-product of some herbicides, are potent inducers of the enzyme (6) and may therefore exacerbate the metabolic activation of other procarcinogens to carcinogens. In a rat model, chronic treatment with TCDD promoted development of ovarian tumors (7). An industrial accident in Seveso, Italy, in 1976 contaminated the area with TCDD and raised ovarian cancer incidence among female residents (8). Similarly, endogenous factors, particularly estrogens, such as 17β-estradiol (E_2) and estrone (E_1), could be converted into catechol estrogens and other genotoxic metabolites via the action of CYP1A1 as well as CYP1B1 (9, 10). These reactive metabolites are known carcinogens of mammary cells (10) and may also be involved in the neoplastic transformation of HOSE cells, which are exposed to high levels of follicular estrogens associated with ovulation (11, 12). In this regard, women who carry polymorphic variants that confer higher CYP1A1 enzyme activity, such as the Ile/Val or Val/Val polymorphism in exon 7 (13), are at higher risk for ovarian cancer (14, 15). Additionally, positive interactions have been shown between tobacco smoking and *CYP1A1* (*Msp*I) polymorphism (16) as well as between high caffeine consumption and Ile/Val polymorphism (14) in ovarian cancer patients. Based on findings from these studies, we hypothesized that CYP1A1 plays a key role in mediating the carcinogenicity of specific endogenous and exogenous chemicals on the ovarian surface epithelium.

Alternative splicing is an important mechanism for generating proteomic complexity and functional diversity (17). Removal of intron sequences from pre-mRNA is carried out by a ribonucleoprotein complex called a spliceosome. Most splicing events occur where the intron starts with GT and ends with AG, the so-called GT-AG rule. However, completion of the Human Genome Project has revealed other noncanonical splice pairs, including AT-AC (18), along with novel spliceosomes (19). New categories of alternative splicing events, including insertion of cryptic exons or excision of cryptic intron, production of exon/intron isoforms, and intron retention, have also been characterized (20, 21). However, few of these new splicing mechanisms have been directly implicated in the pathogenesis of cancers.

In this study, we identified a novel *CYP1A1* variant (*CYP1A1v*) that is formed via excision of an 84-bp cryptic intron within exon 2 of the gene. Thus, the goals of this study were (*a*) to compare

Note: K-M. Lau is currently at the Department of Anatomical and Cellular Pathology, Faculty of Medicine, Chinese University of Hong Kong, Shatin, New Territories, Hong Kong, China. J. Mobley is currently at the Department of Biochemistry, Vanderbilt University, Nashville, TN 37235.

Requests for reprints: Shuk-Mei Ho, Department of Surgery, University of Massachusetts Medical School, Lazare Research Building, Room 504, 364 Plantation Street, Worcester, MA 01605-2324. Phone: 508-856-1909; Fax: 508-856-8699; E-mail: shuk-mei.ho@umassmed.edu.

the expression levels of *CYP1A1wt* and *CYP1A1v* in normal HOSE cell lines to those in ovarian cancer cell lines, (*b*) to investigate the expression pattern of CYP1A1 in 30 cases of clinical specimens, (*c*) to determine whether CYP1A1v is enzymatically active and compare its subcellular distribution with that of CYP1A1wt, and (*d*) to assess whether these isoforms possess transforming potentials when expressed stably in HOSE cell lines in the absence or presence of procarcinogens, such as benzo(*a*)pyrene (BaP, a prototype PAH) and estrogen (E_2, an endogenous estrogen). Our findings showed that both CYP1A1 isoforms are overexpressed in ovarian cancer cell lines and clinical specimens. Importantly, CYP1A1v was found to be enzymatically active and exclusively localized to the mitochondria and nucleus. Forced expression of either isoforms induced anchorage-independent growth in HOSE cells, especially in the presence of BaP and E_2. Collectively, these data provided the first evidence that CYP1A1 overexpression and alternative splicing could contribute to ovarian cancer initiation and progression.

Materials and Methods

Cell cultures and cell lines. Four normal primary HOSE cell cultures (HOSE 27, 20, 17, and 13), four immortalized normal HOSE cell lines (HOSE 301, 306, 636, and 646; ref. 22), and four ovarian cancer cell lines (OVCA 420, 429, 432, and 433; ref. 23) were used in this study. These cells were cultured and maintained as reported previously (22–24).

Clinical specimens. Human surgical ovarian tissues were collected by Z.J. at the Department of Pathology, University of Massachusetts Medical School (Worcester, MA) through routine procedures for histologic diagnosis. A total of 28 clinical specimens, including 24 ovarian neoplasms (18 serous adenocarcinomas, 3 mucinous adenocarcinomas, 2 borderline malignant mucinous tumors, and 1 benign serous cystadenoma), 3 normal ovaries, and 1 pancreatic metastasis to ovary, were included in this study. Paraffin-embedded tissue sections were cut at 5 μm and mounted on SuperFrost Plus slides (Erie Scientific, Portsmouth, NH).

Immunohistochemistry. Epitope retrieval of 5 μm paraffin-embedded tissue sections was achieved through the use of antigen unmasking solution (Vector Laboratories, Burlingame, CA). A polyclonal rabbit anti-human CYP1A1 antibody (Human Biologics International, Scottsdale, AZ) with 1:100 dilution was applied. To show specificity of the antibody, pre-absorption experiment was done using recombinant antigen purchased by Clontech (Palo Alto, CA). Routine and standard immunohistochemical procedures were carried out as reported previously (25).

RNA isolation and reverse transcription-PCR analysis. Total RNA was isolated using TRI-reagent (Sigma, St. Louis, MO) according to protocols provided by the manufacturer. The forward primer of *CYP1A1v* recognized the boundary flanking the deletion of the novel variant of *CYP1A1*. Hot-start PCR using AmpliTaq Gold DNA polymerase (Perkin-Elmer, Norwalk, CT) was used in all amplification reactions. The PCR program for *CYP1A1wt* and *CYP1A1v* (CYP1A1-F 5′-AAGCACGTTGCAGGAGCTGATG-3′ and CYP1A1-R 5′-ACATTGGCGTTCTCATCCAGCTGCT-3′), *CYP1A1v* (CYP1A1v-F 5′-GCCTAGTCAACCTGAATGCC-3′ and CYP1A1v-R 5′-CGAAGGAA-GAGTGTCGGAAG-3′), and *CYP1B1* (CYP1B1-F 5′-GGCTGGATTTGGA-GAACGTA-3′ and CYP1B1-R: 5′-TCATCACTCTGCTGGTCAGG-3′) was 30 cycles of 1 minute at 94°C, 1 minute at 65°C, and 1 minute at 72°C, except that glyceraldehyde-3-phosphate dehydrogenase (*GAPDH*; GAPDH-F: 5′-CCACCCATGGCAAATTCCATGGCA-3′ GAPDH-R: 5′-TCTAGACGGCAGGT-CAGGTCCACC-3′) cDNA was amplified at 26 cycles. Signal intensities of *CYP1A1*, *CYP1A1v*, and *CYP1B1* amplimers were normalized to those of *GAPDH* to produce arbitrary units of relative abundance.

Direct DNA sequencing analysis. Reverse transcription-PCR (RT-PCR) products corresponding to *CYP1A1* transcripts (wild-type and variant) were amplified using *CYP1A1* primer sets listed above. The DNA bands of interest were excised and purified and subjected to radiolabeled primer cycle sequencing using the ThermoSequenase cycle sequencing kit (Amersham Biosciences Corp., Piscataway, NJ). Two separate rounds of sequencing were done to ensure reproducibility.

Western blot analysis. Nuclear, mitochondrial, microsomal, and cytosolic fractions were isolated according to the method of Le Ferrec et al. (26). Protein concentrations of each fraction were measured by Bradford assay kit (Bio-Rad, Hercules, CA). Protein (50 μg) was separated on 10% SDS-polyacrylamide gels and electroblotted onto polyvinylidene difluoride membranes. Methods and reagents used in Western blot analyses were described previously (27).

Immunofluorescence staining. All four OVCA cell lines were grown on coverslips to 80% confluence and then stained with 2 μmol/L MitoTracker Red CM-H_2XROS (Molecular Probes, Eugene, OR) in culture medium for 30 minutes. Methods of fixation, permeabilization, and antibody staining were followed as reported previously (28) with following modifications. Goat polyclonal human CYP1A1 antibody (Gentest, Woburn, MA) and chick anti-goat antibody tagged with Alexa Fluor 488 (Molecular Probes) were diluted to 1:100 and 1:1,000, respectively. The control experiment used human CYP1A1 supersomes (Gentest) preabsorbed primary antibody.

Ethoxyresorufin *O*-deethylase activity assay. Ethoxyresorufin *O*-deethylase (EROD) activity in different subcellular fractions from various OVCA cell lines was assessed according to the method of Burke et al. (29). Reaction mixtures composed of 25 μg protein and the NADPH regenerating system were employed. To determine maximal CYP1A1 activity, each sample was assayed concurrently with and without the addition of 1 unit CYP reductase (Sigma).

Generation of stable transfected human ovarian surface epithelium cell lines. Full-length *CYP1A1wt* and *CYP1A1v* cDNAs were amplified using Platinum Taq High Fidelity System (Invitrogen, Carlsbad, CA) and a specific pair of primers (forward primer tgctagcATGCTTTTCCCAATCTC-CAT and reverse primer atttgcggccgcCTAAGAGCGCAGCTGCAT). To facilitate directional cloning of the PCR products, two restriction sites, *Nhe*I and *Not*I, were engineered to the 5′ end of forward and reverse primers, respectively (as shown in small letters). PCR reactions were initiated at 94°C for 3 minutes and followed by 40 cycles of 1 minute at 94°C, 1 minute at 60°C, and 2 minutes at 68°C and continued to incubate at 68°C for 10 minutes at the end of cycle. PCR products were gel purified, digested, and cloned into pcDNA3.1 vector (Invitrogen) to generate *pcDNA-1A1wt* and *pcDNA-1A1v* vectors that express full-length transcripts of *CYP1A1wt* and *CYP1A1v*, respectively. Identity and reading frame of *pcDNA-1A1wt* and *pcDNA-1A1v* were confirmed by DNA sequencing (Macrogen, Inc., Seoul, Korea). Each of the immortalized HOSE cell lines (HOSE 301, 306, 636, and 642) was stably transfected with *pcDNA-1A1wt* and *pcDNA-1A1v*, separately, using LipofectAMINE Plus reagent (Invitrogen). Empty vector was also stably transfected into HOSE cell lines to serve as a control. Stable transfectants of HOSE cell lines carrying the empty vector, *pcDNA-1A1wt*, and *pcDNA-1A1v* were named as CTL, WT, and V, respectively. For each of the four HOSE lines, we generated their respective CTL, WT, and V derivatives.

Soft agar assay. Stable transfected HOSE cells were trypsinized, counted, and mixed with 0.4% Noble agar in complete medium with 5% charcoal-stripped serum (labeled as UT), charcoal-stripped medium with 1 μmol/L estrogen (labeled as E_2), or charcoal-stripped medium with 1 μmol/L BaP at a concentration of 1,250 cells/250 μL and then transferred into a 0.8% Noble agar precoated 24-well plates. Plates were incubated in 2× medium for up to 4 weeks. The number of colonies formed in soft agar for each of the four HOSE cell lines transfected with the same vector was averaged and SDs were calculated.

***In silico* analyses.** Extensive sequence analyses were carried out using nucleotide and protein BLAST programs provided by National Center for Biotechnology Information (http://www.ncbi.nlm.nih.gov). DNA sequences comparison was done using Clustalw from European Bioinformatics Institute (http://www.ebi.ac.uk/clustalw). Possible signal sequences and the hydrophilicity/hydrophobicity of CYP1A1 protein were analyzed using PSORTII (http://psort.ims.u-tokyo.ac.jp/form2.html) and SwissProt from Swiss Institute of Bioinformatics (http://us.expasy.org/), respectively.

Statistical analyses. One-way ANOVA was used to detect significant differences among the various group means. A multiple range test using the Tukey-B procedure was employed to compare the individual group means. Significance was set at $P < 0.05$ or 0.01.

Results

Identification of a novel *CYP1A1v* in OVCA cells. In our initial experiments, when RT-PCR analyses were conducted using a primer set designed for *CYP1A1*, two PCR products of different sizes were detected in cDNA samples prepared from OVCA cells (Fig. 1*A*): a 387-bp product expected to be amplified from wild-type *CYP1A1* transcripts and a smaller (303 bp) product. To minimize the chances of PCR artifacts, a more stringent annealing temperature (65°C) was used for all subsequent PCRs. The smaller-sized fragment was consistently amplified from all reactions under these conditions. DNA from the smaller band was isolated and sequenced, revealing that it could be derived from transcripts of a splicing variant. When compared with the wild-type transcript, the splicing variant has an 84-bp deletion in exon 2 (Fig. 2*A*). To our knowledge, its sequence had never been reported. We therefore concluded that it is a novel splicing variant, which we here called *CYP1A1v.* This sequence has since been deposited in Genbank with the assigned accession no. AY310359. A new set of specific primers designed to amplify *CYP1A1v* covering the variant-specific exon junction was used for subsequent semiquantification of the variant transcripts.

Overexpression of *CYP1A1wt* and the novel *CYP1A1v* in OVCA cells compared with human ovarian surface epithelium cells. Semiquantitative RT-PCR analyses showed that primary cultures of normal HOSE cells and immortalized HOSE cell lines expressed minimal levels of *CYP1A1wt* mRNA and *CYP1A1v* mRNA (Fig. 1*A* and *B*). In contrast, the four OVCA cell lines consistently showed overexpression of the two *CYP1A1* transcripts compared with levels found in HOSE cell cultures. About a 5-fold increase in the *CYP1A1wt* mRNA and a 10-fold increase in *CYP1A1v* mRNA were observed in the OVCA cell lines on average (Fig. 1*B*). In contrast, there was no observable difference in *CYP1B1* mRNA expression levels among the various HOSE and OVCA cell lines.

Overexpression of CYP1A1 protein and atypical nuclear staining in human ovarian cancer specimens. A total of 27 clinical specimens, including 24 ovarian neoplasms (18 serous adenocarcinomas, 3 mucinous adenocarcinomas, 2 borderline malignant mucinous tumors, and 1 benign serous cystadenoma) and 3 normal ovaries were immunostained with a polyclonal rabbit anti-human CYP1A1 antibody to assess their expression of CYP1A1 proteins (Fig. 3). Strong cytoplasmic (nonnuclear) staining was restricted to the cancer cells of serous and mucinous adenocarcinomas but was more widespread in stromal cells (Fig. 3*A-C*). Some cancer cells in these specimens showed both cytoplasmic and nuclear staining (Fig. 3*B*). CYP1A1 protein was also immunolocalized in the epithelial cells of borderline mucinous lesions (Fig. 3*A*). The majority of serous and mucinous carcinoma cells showed immunopositivity in both nuclei and cytoplasmic staining (Table 1). Expression of cytoplasmic and nuclear CYP1A1 seems to decline concomitantly in types of carcinoma with lower malignancy. CYP1A1 immunonegativity was detected in benign serous cystadenoma (Fig. 3*D*) and normal human ovary. The one human tissue specimen of pancreatic metastasis to ovary in this study showed no detectable CYP1A1 protein expression (data not shown).

Overexpression of CYP1A1wt protein and CYP1A1v protein in ovarian cancer cell lines and exclusive localization of CYP1A1v in cell nucleus and mitochondria. Western blot analyses revealed that wild-type and variant CYP1A1 protein were expressed at very low levels in HOSE cells but were abundant in OVCA cell lines (Fig. 4*A*). Subcellular fractionation of OVCA cells revealed that the wild-type and variant proteins are localized in different cellular compartments. CYP1A1wt was principally associated with the microsomal fraction, whereas CYP1A1v resided predominantly in the nuclear and mitochondrial compartments of OVCA cells (Fig. 4*A*). The unique subcellular distribution of CYP1A1v is specific, because no wild-type enzyme was colocalized to these fractions. Interestingly, neither protein was detected at any significant level in the cytosolic fraction. The unusual localization of CYP1A1v in the nucleus and mitochondria was also confirmed by immunofluorescence microscopy (Fig. 4*B*). The fluorescence signals of CYP1A1 immunoreactivity (Fig. 4*B*, *2*) completely coincided with signals from nuclear (*blue*; Fig. 4*B*, *1*) and mitochondrial (*red*; Fig. 4*B*, *3*) trackers in contrast to the results obtained with an

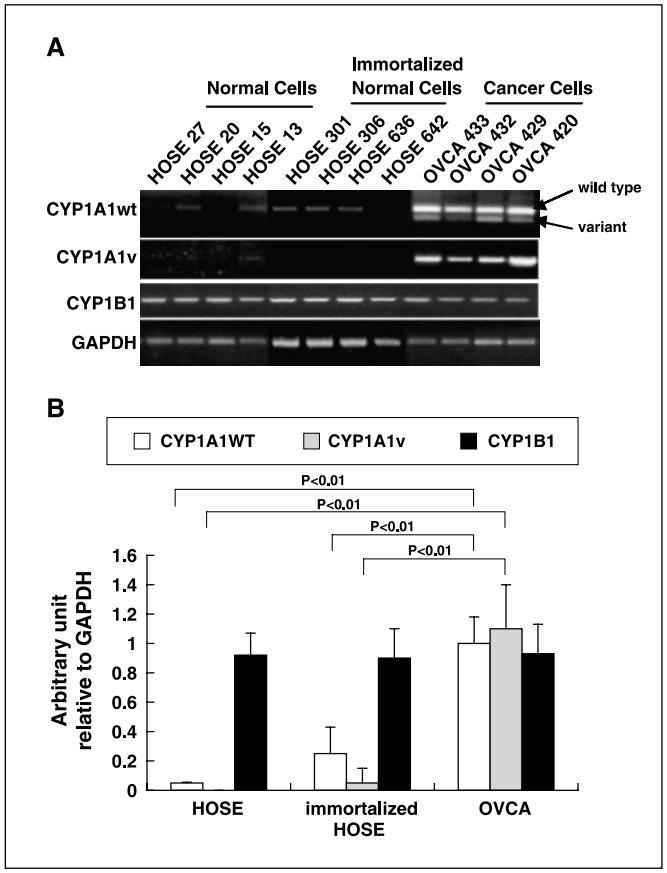

Figure 1. *A,* relative abundance of *CYP1A1wt*, *CYP1A1v*, *CYP1B1*, and *GAPDH* transcripts in different normal, immortalized normal, and ovarian cancer cells. RT-PCRs were done on 1 μg RNA using primer sets for corresponding genes. Representative fluorographs of the RT-PCR products. Bottom bands appearing exclusively in cancer cells were purified and sequenced. *B,* relative abundance of *CYP1A1wt* (*white*), *CYP1A1v* (*gray*), and *CYP1B1* (*black*) transcripts in HOSE and OVCA cells. *Columns,* mean relative abundance of gene transcripts from all primary cultures of normal and immortalized HOSE cells and those from the four OVCA cell lines [$n = 12$ (HOSE); $n = 12$ (immortalized HOSE); and $n = 12$ (OVCA)]; *bars,* SD. One-way ANOVA was applied to calculate the statistical significance of *CYP1A1wt* and *CYP1A1v* mRNA expression among HOSE, immortalized HOSE, and OVCA samples ($P < 0.01$).

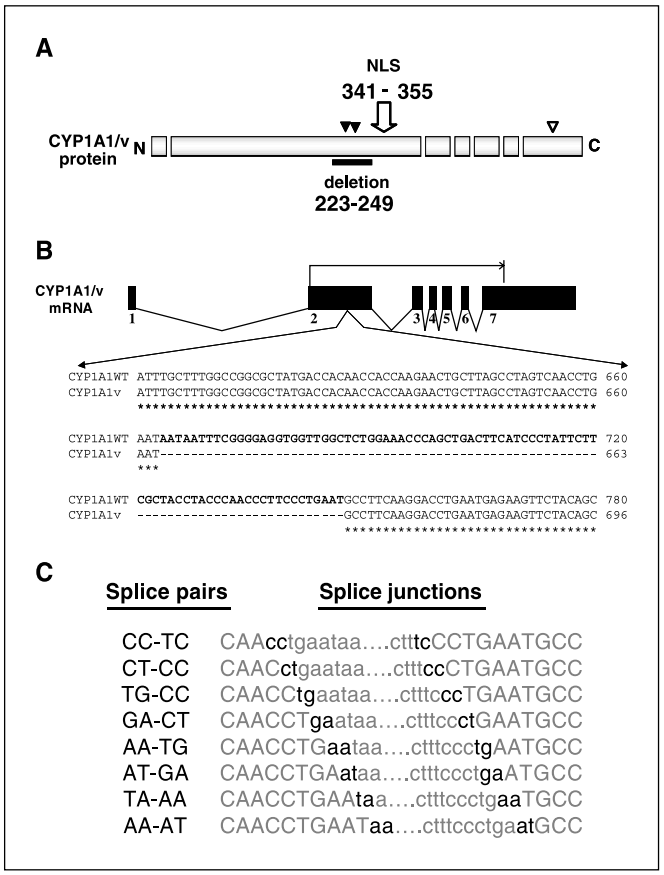

Figure 2. Schematic diagram showing CYP1A1v protein and mRNA. *A,* location of 28–amino acid residues (*deletion*) and NLS. ▼, amino acids 224 and 228 in helix F were deleted from the variant; ▽, hotspot (amino acid residue 462) of CYP1A1 polymorphism. *B,* Clustalw alignment of CYP1A1v against CYP1A1wt. The deleted cDNA region (84 bp) is highlighted (*bold*) in the CYP1A1wt sequence. *Right,* cDNA positions of both wild-type and variant transcripts. *C,* eight possible modes of processing *CYP1A1* pre-mRNA. Various donor and acceptor splice sites are highlighted.

antibody preparation preabsorbed with the antigen (Fig. 4*B*, *6*). The low levels of CYP1A1 signal observed in the nonmitochondrial compartment of the cytoplasm (Fig. 4*B*, *4* and *8-10*) could be due to association of CYP1A1wt with the microsomes.

Computer-aided analysis of the *CYP1A1v* sequence. Analysis of the full-length sequence revealed that the 84-bp deletion is in-frame and would not cause premature termination (Fig. 2*B*), implying that the variant protein will have 28 fewer amino acid residues (amino acids 223-249; Fig. 2*A*) in its NH_2-terminal region than the wild-type protein. An extensive Genbank search found no previous report of the variant. However, a human EST clone (CB267342) in an adipocyte cDNA library was found to correspond to our reported sequence of the variant. This evidence strongly supports our belief that CYP1A1v exists in some other tissues and is not an artificial PCR product.

By comparing the sequence of *CYP1A1v* mRNA to that of the wild-type transcript, eight possible splice junction pairs were recognized (i.e., the dinucleotides upstream and downstream of the splice site could be CC-TC, CT-CC, TG-CC, GA-CT, AA-TG, AT-GA, TA-AA, or AA-AT; Fig. 2*C*). However, none of these obeyed the GT-AG rule (30), suggesting that a non-canonical splice site is responsible for alternative splicing of the *CYP1A1* pre-mRNA. Moreover, among the eight possible sites, because only one splice junction pair, AA-AT, has been suggested to exist by statistical analysis of all annotated genes in the mammalian genome (18), it may be the pair involved in splicing of this variant.

To investigate why only the CYP1A1v (not the wild-type protein) is targeted to the nucleus and mitochondria, an extensive *in silico* search of possible signaling peptides was done. A putative bipartite basic nuclear localization signal (NLS) was identified in the CYP1A1 amino acid sequence from residues 341 to 357 (RKIQEELDT-VIGRSRRP; Fig. 2*A*), which matches the consensus motif $(K/R)_2X_{10\text{-}12}(K/R)_3$ of nucleoplasmin (31). However, these searches failed to identify a mitochondrial matrix-targeting signal, most commonly composed of positive charge and hydroxylated residues (32), in the CYP1A1v. Of interest, hydrophobicity analysis revealed a decrease in the overall hydrophobicity in the NH_2-terminal region of CYP1A1, most markedly around amino acids 230 to 260, which encompasses the deleted region (33). Thus, perturbation in this general area may result in the formation of a functional mitochondrial targeting signal.

According to a recent molecular modeling study of human CYP1A1 (34), both resorufins and BaP are primarily stabilized by hydrophobic interactions in the substrate binding pocket. Within this substrate binding pocket, two key amino acid residues in helix F responsible for substrate stabilization (amino acids 224 and 228; Fig. 2*A*) were found to be deleted from the CYP1A1v. Loss of these amino acids may result in alterations in substrate specificity and/or binding affinity in the variant protein.

CYP1A1v in both nucleus and mitochondria is active in ethoxyresorufin *O*-deethylase assay. To determine whether the mitochondria- and nucleus-localized CYP1A1 protein, presumably derived from the *CYP1A1v*, is catalytically active, the EROD assay was done after subcellular fraction of ovarian cancer cell lines (OVCA 429, 432, and 433) in the presence and absence of exogenous CYP oxidoreductase. The enzyme activity found in subcellular fractions of each cell lines were determined and averaged (Fig. 5). In the absence of exogenous CYP oxidoreductase, the highest EROD activity was detected in the nuclear fraction followed by the mitochondrial and microsomal fractions, whereas the cytosolic fraction was devoid of EROD activity. In the presence of extra CYP oxidoreductase, significantly higher levels (3- to 4-fold increases) of EROD activities were found in all fractions. The greatest increase was observed in the microsomal fraction followed by the mitochondrial and nuclear fractions. Under this condition, a low level of cytosolic EROD activity was also detected. We noticed that NAPDH oxidoreductase plays a greater role in enhancing the enzyme activity of CYP1A1wt and CYP1A1v in ovarian cancer cell lines. It seems that the activities of both CYP1A1wt and CYP1A1v are limited by low levels of oxidoreductase activity in ovarian cancer cells when compared with TCDD-stimulated MCF-7 cells (data not shown). Because we have shown exclusive localization of the CYP1A1v in the mitochondria and nucleus by Western blotting, together with previously reported association of CYP1A1wt with the microsomes (35), the EROD data now strongly support the notion that the CYP1A1v is catalytically as active as CYP1A1wt.

CYP1A1wt and CYP1A1v are both involved in benzo(*a*)pyrene- or 17β-estradiol-induced cellular transformation. This experiment sought to determine (*a*) whether overexpression of *CYP1A1wt* and *CYP1A1v* in HOSE cells also results in their protein products localized to different cellular compartment, (*b*)

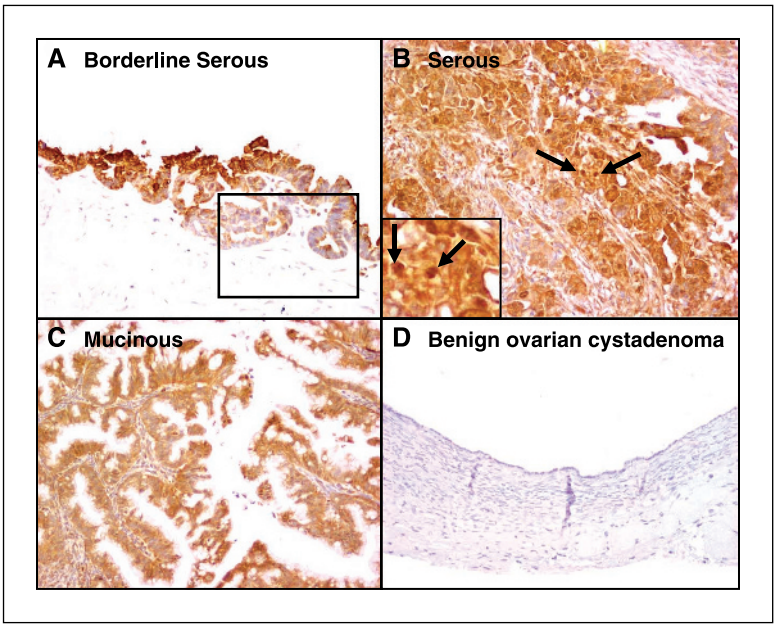

Figure 3. Immunohistochemical stains for CYP1A1 on human ovarian tumors. *A,* serous tumors of borderline malignancy (of low malignant potential) showing positive (*brown*) staining for CYP1A1 in tumor epithelial cells and negative staining in adjacent stroma (*boxed area*). *B,* poorly differentiated serous adenocarcinoma showing cytoplasmic staining and nuclear staining for CYP1A1 in cancer cells (*arrows* and *inset*). *C,* mucinous adenocarcinoma also showing expression of CYP1A1. *D,* benign ovarian cystadenoma was CYP1A1 immunonegative. All sections were counterstained with hematoxylin.

whether overexpression of *CYP1A1wt* or *CYP1A1v* induces neoplastic transformation per se in HOSE cells, and (*c*) whether overexpression of the enzyme mediates cellular transformation caused by an endogenous/exogenous procarcinogen. The soft agar colony formation assay was used to measure acquisition of anchorage-independent growth potential in the four HOSE cell lines (HOSE 301, 306, 636, and 646), each stably transfected with empty *pcDNA3.1* (HOSE-CTL), *pcDNA-1A1wt* (HOSE-WT), or *pcDNA-1A1v* (HOSE-V). BaP, a major PAH produced during cigarette smoking (36), was used as a prototype exogenous environmental procarcinogen. E_2, the major circulating and follicular estrogen, was chosen for our study because ovarian surface epithelial (OSE) cells are often exposed to high levels of this steroid around ovulation or when trapped in the stroma as inclusion cysts (11). Both BaP and E_2 are the known substrates for CYP1A1, and their metabolites are carcinogenic (9, 10, 37).

All four HOSE-CTL cell lines expressed no detectable *CYP1A1wt* or *CYP1A1v* mRNA as shown by semiquantification of the transcripts by RT-PCR (Fig. 6*A*). As expected, HOSE-V cell lines expressed high levels of *CYP1A1v* transcript and no detectable *CYP1A1wt* mRNA (Fig. 6*A*, *top*). Surprisingly, HOSE-WT cell lines, in addition to high levels of *CYP1A1wt* mRNA, also expressed detectable levels of *CYP1A1v* transcripts, likely products of alternative splicing of the wild-type transcript (Fig. 6*A*, *middle*). Exposure of HOSE cell lines (CTL, WT, or V) to BaP and E_2 did not alter expression levels of *CYP1A1wt*, *CYP1A1v*, or *CYP1B1*.

Two approaches were used to determine whether HOSE-WT and HOSE-V cell lines overexpressed the CYP1A1s that exhibited extra–endoplasmic reticulum (ER) localization. EROD assays were done on subcellular fractions of three types of stable transfected HOSE cell lines (HOSE-CTL, HOSE-WT and HOSE-V) and revealed the following: (*a*) the enzyme activities of CYP1A1 were elevated in

Table 1. Expression of CYP1A1 in ovarian carcinoma

Type of tumors	No. cases	Cytoplasmic staining*			Nuclear staining		
		<75%	30-75%	>30%	<75%	30-75%	>30%
Serous cancer	20	11	9	0	4	10	6
Mucinous cancer	5	4	1	0	1	4	0
Serous, low malignant potential (of borderline malignancy)	3	2	1	0	1	2	0
Mucinous, low malignant potential (of borderline malignancy)	2	0	2	0	0	1	1
Total	30	17 (57%)	13 (43%)	0 (0%)	6 (20%)	17 (57%)	7 (23%)
			100%			100%	

*Nonnuclear region includes mitochondria, microsomes, and cytosol.

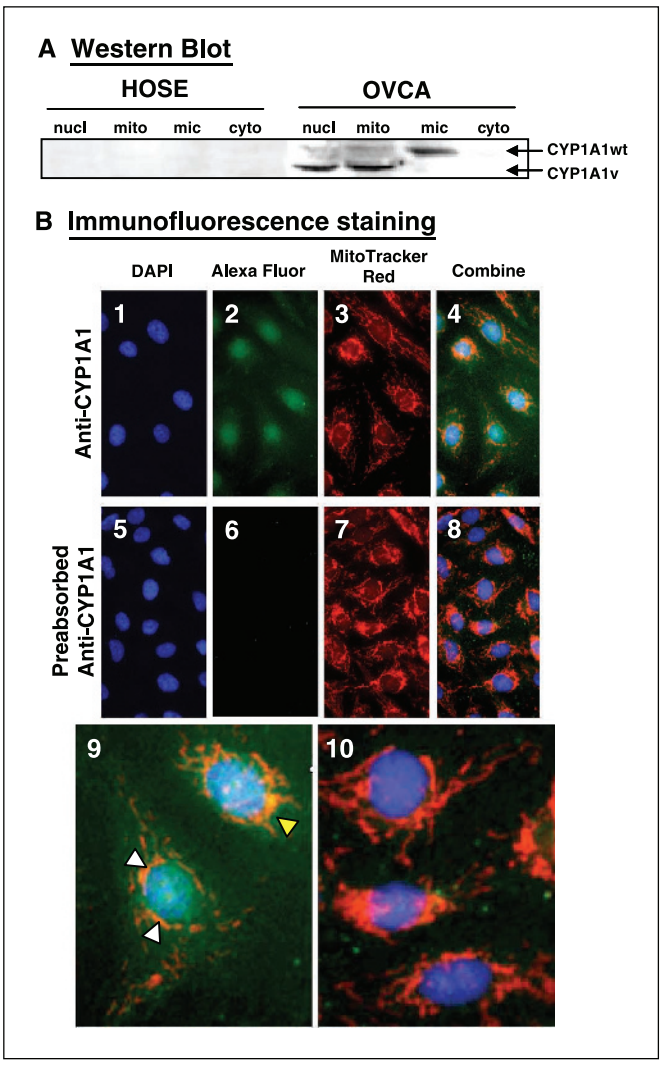

Figure 4. *A,* Western blot analysis of CYP1A1 in various subcellular fractions of HOSE and OVCA cells. Representative experiment. *nucl*, *mito*, *mic*, and *cyto,* fractions isolated from nucleus, mitochondria, microsomes, and cytosol, respectively. CYP1A1v is uniquely found in nucleus and mitochondria, whereas CYP1A1wt resides in microsomes. *B,* immunofluorescence staining. *1* and *5* (*blue*), 4′,6-diamidino-2-phenylindole (*DAPI*) staining; *2* (*green*), anti-CYP1A1 antibody staining; *6,* antigen preabsorbed anti-CYP1A1 antibody staining; *3* and *7* (*red*), MitoTracker Red staining; *4* and *8,* composite images of *1* to *4* and *5* to *8*, respectively; *9,* magnified version of *4* showing the differential staining of CYP1A1 in mitochondria (*orange*) in white arrowheads and microsomes (*green*) in yellow arrowheads; *10,* magnified version of negative control (*8*) using preabsorbed antibody.

both HOSE-WT and HOSE-V cell lines when compared with HOSE-CTL cells, (*b*) the enzyme activities were predominantly detected in the nuclear fractions (Fig. 6*B*), and (*c*) little to no enzymatic activities were present in the mitochondrial fraction. Results from immunofluorescence assays (data not shown) confirmed this observation. Of interest to note, the quantity of mitochondria in those HOSE cell lines was extremely low when compared with OVCA cells (data not shown).

As shown in Fig. 6*C*, the soft agar assay revealed that (*a*) exposure of HOSE cell lines transfected with the empty vector (HOSE-CTL) to the procarcinogens BaP and E_2 did not cause significant increases in soft agar colony formation potentials in these cell lines, (*b*) stable transfection of HOSE cell lines with *pcDNA-1A1wt* or *pcDNA-1A1v* vector significantly increased their soft agar colony formation potentials by 100% to 200% ($P < 0.01$) in the absence of BaP or E_2 exposure, and (*c*) after exposure to BaP or E_2 HOSE-WT and HOSE-V cell lines exhibited additional increases in soft agar colony formation potentials; the effect of E_2 was greater than that of BaP in both kinds of stable transfectants and greatest in HOSE-WT cell lines.

Discussion

In this study, we identified a novel *CYP1A1v* produced by a splicing event that involves an excision of an 84-bp cryptic intron. CYP1A1v, which is enzymatically active and is uniquely and exclusively located in the nucleus and the mitochondria instead of in the ER, where the wild-type enzyme resides. Importantly, when HOSE cells were engineered to overexpress *CYP1A1wt*, this alternative splicing mechanism generated *CYP1A1v* from the mature wild-type transcript. Hence, an overall increase in *CYP1A1* gene expression would give rise to both transcripts and proteins and extend cellular localization of the enzyme to new cellular compartments. Of significance, we detected higher levels of *CYP1A1wt* and *CYP1A1v* mRNA in four ovarian cancer cell lines when compared with primary cultures of normal HOSE cells and four immortalized HOSE cell lines, which express little or no *CYP1A1* transcripts. Immunocytochemistry revealed overexpression of the enzyme in various types of ovarian cancers with both cytosolic and nuclear localization. Comparable levels of CYP1A1 activity, as measured by the EROD assay, were found in nuclear, mitochondrial, and microsomal fractions of OVCA cells but not in HOSE cells. Enzyme activity in all three compartments depended on NADPH regeneration. Further investigation showed acquisition of anchorage-independent growth in HOSE cells engineered to stably overexpress exogenous *CYP1A1wt* or *CYP1A1v*. On exposure of these cells to BaP or E_2 (especially to the steroid, E_2), further enhancement of anchorage-independent growth was observed. Taken together, these findings provide strong support for an essential role of CYP1A1 in neoplastic transformation of HOSE cells likely via metabolic activation of exogenous/endogenous procarcinogens and utilization of a unique alternative splicing mechanism to broaden the distribution of the enzyme to critical organelles. The overall hypothesis of this study has been summarized in Fig. 7.

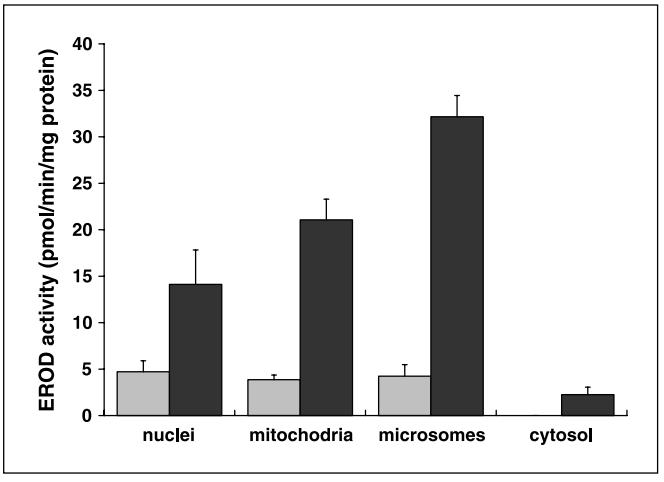

Figure 5. EROD activity in different subcellular fractions of OVCA cells. *Gray* and *black columns,* reaction in the absence or presence, respectively, of exogenous CYP oxidoreductase. *Columns,* average of measurements from four OVCA cell lines; *bars,* SD.

Splicing events have been characterized and divided into four different categories (20, 21): insertion of cryptic exons or excision of crytic introns, production of exon/intron isoforms, and intron retention. In our study, an 84-bp cryptic intron is spliced from exon 2 of *CYP1A1wt*, possibly via an AA-AT splice junction pair, as suggested by our *in silico* analysis. This is a noncanonical splice pair, because >96% of pre-mRNA splicing use the conservative GT-AG pair (18). The involvement of noncanonical splice junction pairs may be due to poorly conserved 5′ and 3′ splice sites and/or many cryptic splice sites (38). Recent findings suggest that introns flanked by another noncanonical AT-AC pair are excised by a spliceosome composed of nonclassic types of small nuclear ribonucleoproteins (19). Interestingly, when HOSE cells are stably transfected with a *CYP1A1wt* expression vector, we found that *CYP1A1v* coexisted with the wild-type transcript. This finding indicates that the mature transcripts of *CYP1A1wt* are susceptible to this splicing event. Thus, induction of *CYP1A1wt* overexpression in normal OSE cells by xenobiotic/endobiotics or physiologic stresses could yield both transcripts along with their protein products and might extend the coverage of enzyme to new cellular organelles, where they may contribute to an imbalance in activation/detoxification of procarcinogens. This splicing event may exist in tissues other than the OSE because we also observed expression of *CYP1A1v* mRNA in breast and prostate cancer cells.[5]

Although a few early reports detected CYP1A1-like enzyme activity in cell nucleus (39) and mitochondria (40) in rodent models, the enzyme identities remain unclear. *CYP1A1v* is the first human CYP1A1v to be identified and characterized at both molecular and biological levels. Thus, alternative splicing of *CYP1A1* could be considered a mechanism for targeting the enzyme to extra-ER locales. Computational analyses identified a putative bipartite basic NLS, which is masked in the CYP1A1wt. One can speculate that removal of the cryptic intron results in the activation of this NLS and nuclear targeting of CYP1A1v. However, we cannot yet explain the acquisition of the mitochondrial matrix targeting signal via deletion of the 84-bp region, except to hypothesize that the deletion induces an increase in hydrophobicity in the NH_2 terminus of the molecule and creates a mitochondrial targeting signal (32) for the variant enzyme. Most of the CYP enzymes residing in the ER have been shown to depend on NADPH-oxidoreductase for electron transfer (41), and their activities are enhanced in the presence of an NADPH regenerating system. Here, we found that the EROD activity in the mitochondrial, nuclear, and microsomal fractions of ovarian cancer cells were all elevated in the presence of exogenous NADPH-oxidoreductase, suggesting that comparable cofactor requirements exist between the wild-type and the variant enzyme.

Our results strongly support a role for aberrant expression of CYP1A1 in ovarian carcinogenesis. Exposure of HOSE cells to BaP or E_2 per se did not induce increased expression of the enzyme. In the absence of CYP1A1 expression, these two procarcinogens were ineffective in inducing an anchorage-independent growth phenotype in these cells. In marked contrast, overexpression of *CYP1A1wt* or *CYP1A1v* in HOSE cell lines significantly increased anchorage-independent growth potentials of HOSE cells even in the absence of BaP or E_2. Elevated levels of *CYP1A1wt* and/or *CYP1A1v* expression probably had caused neoplastic transformation via activation of procarcinogens existing in the culture medium per se. Exposing the

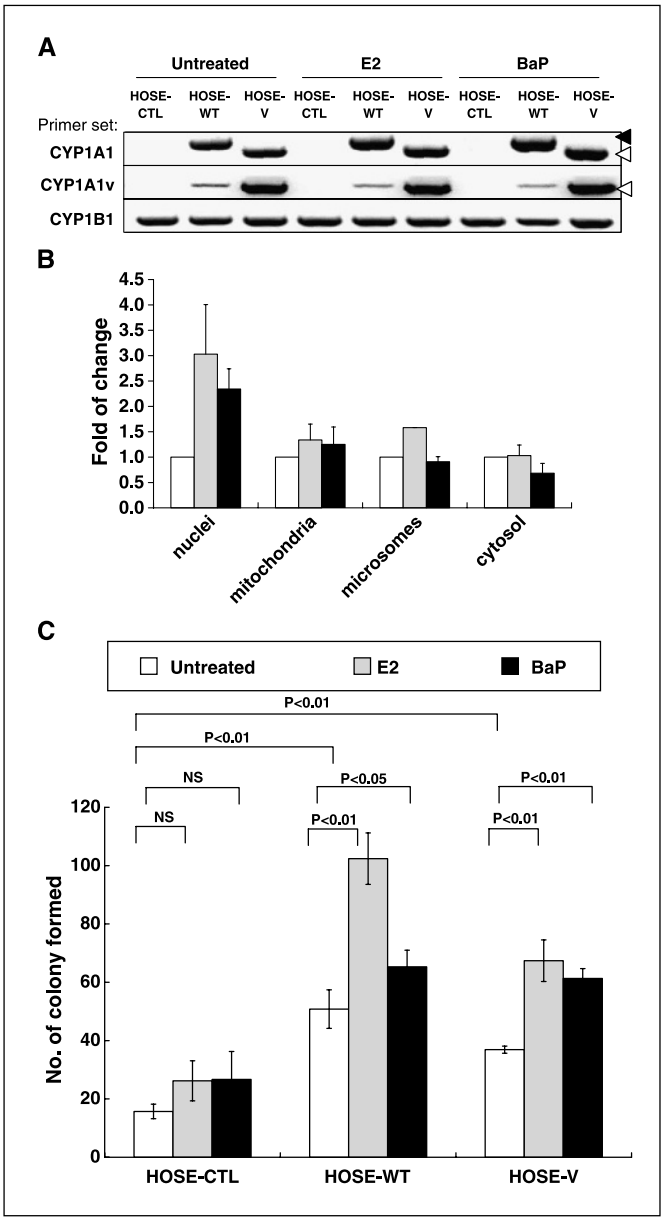

Figure 6. *A,* expression of *CYP1A1wt*, *CYP1A1v*, and *CYP1B1* in a representative HOSE cell line stably transfected with the empty vector (*CTL*), the expression vector for *CYP1A1wt* (*WT*), or one for *CYP1A1v* (*V*) after a 24-hour treatment with 1 μmol/L estrogen (*E2*), 1 μmol/L BaP, or vehicle (*Untreated*), respectively. RT-PCR was done using the *CYP1A1* primer pair that amplifies both wild-type (*solid arrowhead*) and variant (*close arrowhead*) *CYP1A1* transcript (CYP1A1, *top*). The *CYP1A1v*-specific primer pair was used to amplify the variant only (CYP1A1v, *middle*) and the *CYP1B1*-specific primer set for the *CYP1B1* mRNA (CYP1B1, *bottom*). *B,* HOSE cell lines stably transfected with empty vector (HOSE-CTL, *white columns*), the *CYP1A1wt* expression vector (HOSE-WT, *gray columns*), or the *CYP1A1v* expression vector (HOSE-V, *black columns*) were subfractionated by differential centrifugation. Different fractions of HOSE-CTL, HOSE-WT, and HOSE-V cell extracts were obtained and EROD assay was done. Experiments were done as suggested in Materials and Methods. Average fold of change and experiment was done in triplicate. *C,* anchorage-independent growth potentials were measured as number of colonies formed in soft agar for HOSE cell lines stably transfected with empty vector, the *CYP1A1wt* expression vector, or the *CYP1A1v* expression vector. *White*, *gray*, and *black columns,* results for HOSE cell lines stably transfected with the empty pcDNA3.1, pcDNA-1A1wt, or pcDNA-1A1v vector, respectively. *Untreated*, *E2*, and *BaP,* three types of stable transformed HOSE cell lines in soft agar exposed to medium alone, medium with 1 μmol/L E_2, or medium with 1 μmol/L BaP, respectively. *Columns,* mean number of colonies formed in soft agar from all stable transfectants from all four HOSE cell lines; *bars,* SD. One-way ANOVA was applied to calculate the statistical significance among different groups.

[5] Unpublished data.

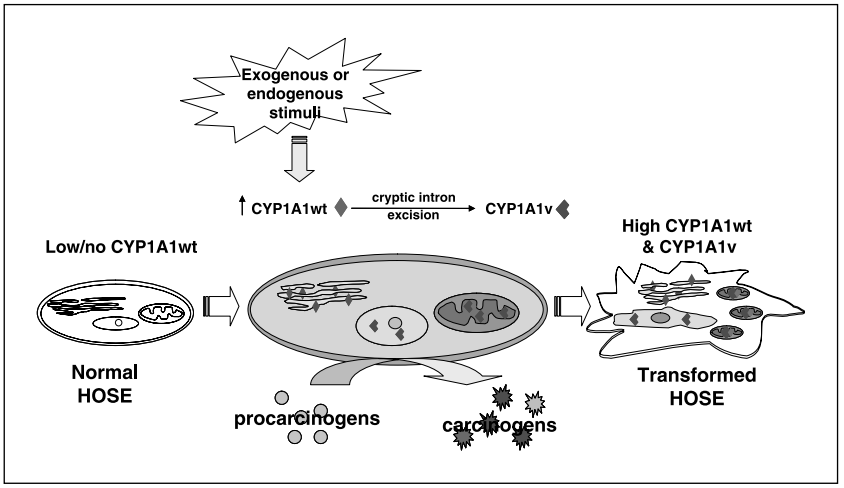

Figure 7. Schematic diagram summarizing the hypothesis of this study. In normal HOSE cells, the expression level of *CYP1A1wt* (*diamond*) is low or undetectable. On exogenous (environmental factors) or endogenous (hormone factors) stimuli, CYP1A1wt can be significantly induced in HOSE cells. Some of the *CYP1A1wt* transcripts can be partially converted into *CYP1A1v* (*broken diamond*) by alternative splicing via cryptic intron excision. The protein products of *CYP1A1v* mRNA are targeted to nucleus and mitochondria instead of microsomes (ER) where CYP1A1wt resides. Both CYP1A1wt and CYP1A1v can metabolize various kinds of procarcinogens into highly reactive carcinogens, which in turn attack protein and DNA within their compartments. As a result of DNA adduct formation, DNA mutations accumulate and eventually impair genome stability. HOSE can be finally transformed with more cancer phenotypes. With the perpetual stimulation of activated carcinogens, transformed cells may progress to more advanced stage.

stable transfectants to BaP or E_2 increased soft agar colony formation in both HOSE-WT and HOSE-V cell lines. Of interest is the marked elevation of soft agar colony formation in HOSE-WT cell cultures exposed to E_2 when compared with HOSE-V cell lines. In contrast, BaP elicited roughly the same response in both types of stable transfectants. Because the overexpression of CYP1A1 in HOSE-WT and HOSE-V cell lines were localized primarily in nuclear compartment possibly due to low abundance of mitochondria in these cell lines, we suggest that nuclear localization of CYP1A1 is sufficient to mediate BaP-induced neoplastic transformation, whereas the E_2-induced transformation may involve the presence of the enzyme in multiple subcellular organelles. Indeed, BaP carcinogenicity is believed to be mediated by the translocation of the procarcinogen to the cell nucleus followed by formation of the mutagenic metabolite BaP-7,8-diol 9,10-epoxide and DNA adducts, which in turn initiate mutagenesis (42, 43).

On the contrary to BaP, estrogen carcinogenicity is much more complex and involves multiple phase I and II enzymes with different subcellular locales. Estrogens are converted to catecholestrogens (2-OH and 4-OH estrogens) and estrogen quinones, which are genotoxic, via CYP1A1 and CYP1B1 metabolic activation (9, 10). Catechol-*O*-methyltransferase catalyzes the methylation of catechol estrogens to methoxyestrogens, which may reduce the potential for genomic damage and suppress cell proliferation via enhancement of 2-MeOE2 formation (44, 45). Aberrant or altered expression of these estrogen metabolic enzymes is implicated in the initiation of human breast and endometrial tumors (9, 10, 46, 47). Analogous information has been scarce for ovarian carcinogenesis. The human ovarian epithelium is routinely exposed to high levels of estrogens such as those produced during the follicular phase of each female cycle. Alternatively, the ovarian epithelium is exposed to abnormal levels of stromal estrogens with the formation of inclusion cysts, which in fact have been proposed as the origin of epithelial ovarian cancer (48). In general, CYP1A1 produces mostly 2-OH estrogens, but a significant amount of 4-OH estrogens is generated simultaneously (49). It has been shown that 4-OH estrogens are more carcinogenic than 2-OH estrogens in a mammary epithelial cell model (10). Whether a similar scenario exists for OSE remains to be investigated in future experiment.

In summary, we here provide the first evidence that *CYP1A1* is overexpressed in ovarian cancer cell lines and ovarian cancers. We also report the identification of a novel variant of CYP1A1 that is enzymatically active and resides exclusively in cell nucleus and mitochondria. Our data suggest that a noncanonical splice group is responsible for the removal of a cryptic intron from the CYP1A1 transcript. These findings raise the possibility that alternative splicing underlies increased functional diversity of CYP1A1 by increasing its subcellular coverage. They also suggest that chronic or repeated induction of CYP1A1 expression in HOSE cells would result in expression of the enzyme in multiple cellular organelles, leading to an imbalanced detoxification-activation homeostasis of xenobiotics/endobiotics, a mechanism long suspected to induce neoplastic transformation.

Acknowledgments

Received 10/21/2004; revised 2/16/2005; accepted 2/24/2005.

Grant support: NIH/National Cancer Institute award CA94221, Department of Defense/U.S. Army Ovarian Cancer Research Program grant DAMD17-99-1-9563, and Mary Kay Ash Foundation Research Award grant 025-01 (S-M. Ho).

The costs of publication of this article were defrayed in part by the payment of page charges. This article must therefore be hereby marked *advertisement* in accordance with 18 U.S.C. Section 1734 solely to indicate this fact.

We thank Dr. Samuel C. Mok (Brigham and Women's Hospital, Boston, MA) for the HOSE and OVCA cell lines.

References

1. Holschneider CH, Berek JS. Ovarian cancer: epidemiology, biology, and prognostic factors. Semin Surg Oncol 2000;19:3–10.
2. Bosetti C, Negri E, Franceschi S, et al. Diet and ovarian cancer risk: a case-control study in Italy. Int J Cancer 2001;93:911–5.
3. Kuper H, Titus-Ernstoff L, Harlow BL, et al. Population based study of coffee, alcohol and tobacco use and risk of ovarian cancer. Int J Cancer 2000;88:313–8.
4. Marchbanks PA, Wilson H, Bastos E, et al. Cigarette smoking and epithelial ovarian cancer by histologic type. Obstet Gynecol 2000;95:255–60.
5. Jeffy BD, Schultz EU, Selmin O, et al. Inhibition of BRCA-1 expression by benzo[*a*]pyrene and its diol epoxide. Mol Carcinog 1999;26:100–18.
6. Whitlock JP. Induction of cytochrome *P*4501A1. Annu Rev Pharmacol Toxicol 1999;39:103–25.
7. Davis BJ, Mccurdy EA, Miller BD, et al. Ovarian tumors in rats induced by chronic 2,3,7,8-tetrachlorodibenzo-*p*-dioxin treatment. Cancer Res 2000;60:5414–9.
8. Pesatori AC, Consonni D, Tironi A, et al. Cancer in a young population in a dioxin-contaminated area. Int J Epidemiol 1993;22:1010–3.

9. Yager JD. Endogenous estrogens as carcinogens through metabolic activation. J Natl Cancer Inst Monogr 2000;67–73.

10. Russo J, Hasan LM, Balogh G, et al. Estrogen and its metabolites are carcinogenic agents in human breast epithelial cells. J Steroid Biochem Mol Biol 2003;87:1–25.

11. Ho SM. Estrogen, progesterone and epithelial ovarian cancer. Reprod Biol Endocrinol 2003;1:73.

12. Murdoch WJ, Martinchick JF. Oxidative damage to DNA of ovarian surface epithelial cells affected by ovulation: carcinogenic implication and chemoprevention. Exp Biol Med (Maywood) 2004;229: 546–52.

13. Crofts F, Taioli E, Trachman J, et al. Functional significance of different human CYP1A1 genotypes. Carcinogenesis 1994;15:2961–3.

14. Terry KL, Titus-Ernstoff L, Garner EO, et al. Interaction between CYP1A1 polymorphic variants and dietary exposures influencing ovarian cancer risk. Cancer Epidemiol Biomarkers Prev 2003;12: 187–90.

15. Aktas D, Guney I, Alikasifoglu M, et al. CYP1A1 gene polymorphism and risk of epithelial ovarian neoplasm. Gynecol Oncol 2002;86:124–8.

16. Goodman MT, McDuffie K, Kolonel LN, et al. Case-control study of ovarian cancer and polymorphisms in genes involved in catecholestrogen formation and metabolism. Cancer Epidemiol Biomarkers Prev 2001; 10:209–16.

17. Caceres JF, Kornblihtt AR. Alternative splicing: multiple control mechanisms and involvement in human disease. Trends Genet 2002;18:186–93.

18. Burset M, Seledtsov IA, Solovyev VV. Analysis of canonical and non-canonical splice sites in mammalian genomes. Nucleic Acids Res 2000;28: 4364–75.

19. Tarn WY, Steitz JA. Pre-mRNA splicing: the discovery of a new spliceosome doubles the challenge. Trends Biochem Sci 1997;22:132–7.

20. Clark F, Thanaraj TA. Categorization and characterization of transcript-confirmed constitutively and alternatively spliced introns and exons from human. Hum Mol Genet 2002;11:451–64.

21. Haseloff J, Siemering KR, Prasher DC, et al. Removal of a cryptic intron and subcellular localization of green fluorescent protein are required to mark transgenic *Arabidopsis* plants brightly. Proc Natl Acad Sci U S A 1997;94:2122–7.

22. Tsao SW, Mok SC, Fey EG, et al. Characterization of human ovarian surface epithelial cells immortalized by human papilloma viral oncogenes (HPV-E6E7 ORFs). Exp Cell Res 1995;218:499–507.

23. Syed V, Ulinski G, Mok SC, et al. Expression of gonadotropin receptor and growth responses to key reproductive hormones in normal and malignant human ovarian surface epithelial cells. Cancer Res 2001;61:6768–76.

24. Lau KM, Mok SC, Ho SM. Expression of human estrogen receptor-α and -β, progesterone receptor, and androgen receptor mRNA in normal and malignant ovarian epithelial cells. Proc Natl Acad Sci U S A 1999; 96:5722–7.

25. Leav I, Lau KM, Adams JY, et al. Comparative studies of the estrogen receptors β and α and the androgen receptor in normal human prostate glands, dysplasia, and in primary and metastatic carcinoma. Am J Pathol 2001;159:79–92.

26. Le Ferrec E, Lagadic-Gossmann D, Rauch C, et al. Transcriptional induction of CYP1A1 by oltipraz in human Caco-2 cells is aryl hydrocarbon receptor- and calcium-dependent. J Biol Chem 2002;277: 24780–7.

27. Gambone CJ, Hutcheson JM, Gabriel JL, et al. Unique property of some synthetic retinoids: activation of the aryl hydrocarbon receptor pathway. Mol Pharmacol 2002;61:334–42.

28. Wagner S, Chiosea S, Nickerson JA. The spatial targeting and nuclear matrix binding domains of SRm160. Proc Natl Acad Sci U S A 2003;100: 3269–74.

29. Burke MD, Prough RA, Mayer RT. Characteristics of a microsomal cytochrome *P*-448-mediated reaction. Ethoxyresorufin *O*-de-ethylation. Drug Metab Dispos 1977;5:1–8.

30. Mount SM, Steitz JA. Sequence of U1 RNA from *Drosophila melanogaster*: implications for U1 secondary structure and possible involvement in splicing. Nucleic Acids Res 1981;9:6351–68.

31. Nigg EA. Nucleocytoplasmic transport: signals, mechanisms and regulation. Nature 1997;386:779–87.

32. Neupert W. Protein import into mitochondria. Annu Rev Biochem 1997;66:863–917.

33. Black SD, Mould DR. Development of hydrophobicity parameters to analyze proteins which bear post- or cotranslational modifications. Anal Biochem 1991;193: 72–82.

34. Szklarz GD, Paulsen MD. Molecular modeling of cytochrome *P*450 1A1: enzyme-substrate interactions and substrate binding affinities. J Biomol Struct Dyn 2002;20:155–62.

35. Ma Q. Induction of CYP1A1. The AhR/DRE paradigm: transcription, receptor regulation, and expanding biological roles. Curr Drug Metab 2001; 2:149–64.

36. Pryor WA. Cigarette smoke radicals and the role of free radicals in chemical carcinogenicity. Environ Health Perspect 1997;105:875–82.

37. Schwarz D, Kisselev P, Cascorbi I, et al. Differential metabolism of benzo[*a*]pyrene and benzo[*a*]pyrene-7,8-dihydrodiol by human CYP1A1 variants. Carcinogenesis 2001;22:453–9.

38. Maniatis T, Tasic B. Alternative pre-mRNA splicing and proteome expansion in metazoans. Nature 2002; 418:236–43.

39. Bresnick E. Drug metabolism: speculations on the future. Drug Metab Rev 1979;10:311–3.

40. Addya S, Anandatheerthavarada HK, Biswas G, et al. Targeting of NH_2-terminal-processed microsomal protein to mitochondria: a novel pathway for the biogenesis of hepatic mitochondrial P450MT2. J Cell Biol 1997;139:589–99.

41. Nebert DW, Negishi M, Lang MA, et al. The Ah locus, a multigene family necessary for survival in a chemically adverse environment: comparison with the immune system. Adv Genet 1982;21:1–52.

42. Wijnhoven SW, Kool HJ, van Oostrom CT, et al. The relationship between benzo[*a*]pyrene-induced mutagenesis and carcinogenesis in repair-deficient Cockayne syndrome group B mice. Cancer Res 2000;60: 5681–7.

43. Chen SY, Lin JR, Darbha R, et al. Glycine *N*-methyltransferase tumor susceptibility gene in the benzo(*a*)pyrene-detoxification pathway. Cancer Res 2004;64:3617–23.

44. Garner EI, Stokes EE, Berkowitz RS, et al. Polymorphisms of the estrogen-metabolizing genes CYP17 and catechol-*O*-methyltransferase and risk of epithelial ovarian cancer. Cancer Res 2002;62: 3058–62.

45. Millikan RC, Pittman GS, Tse CK, et al. Catechol-*O*-methyltransferase and breast cancer risk. Carcinogenesis 1998;19:1943–7.

46. Kristensen VN, Borresen-Dale AL. Molecular epidemiology of breast cancer: genetic variation in steroid hormone metabolism. Mutat Res 2000;462:323–33.

47. Dawling S, Hachey DL, Roodi N, et al. *In vitro* model of mammary estrogen metabolism: structural and kinetic differences between catechol estrogens 2- and 4-hydroxyestradiol. Chem Res Toxicol 2004;17: 1258–64.

48. Feeley KM, Wells M. Precursor lesions of ovarian epithelial malignancy. Histopathology 2001;38: 87–95.

49. Lee AJ, Cai MX, Thomas PE, et al. Characterization of the oxidative metabolites of 17β-estradiol and estrone formed by 15 selectively expressed human cytochrome *P*450 isoforms. Endocrinology 2003;144: 3382–98.